energies

MDPI

Article

Optimal Scheduling of Energy Storage and Shiftable Loads in Grid-Connected Residential Buildings with Photovoltaic Micro-Installations

Roman Korab [1,*], Marcin Połomski [2] and Tomasz Naczyński [3]

[1] Department of Power Systems and Control, Faculty of Electrical Engineering, Silesian University of Technology, 44-100 Gliwice, Poland
[2] Department of Algorithmics and Software, Faculty of Automatic Control, Electronics and Computer Science, Silesian University of Technology, 44-100 Gliwice, Poland; marcin.polomski@polsl.pl
[3] Joint Doctoral School, Silesian University of Technology, 44-100 Gliwice, Poland; tomasz.naczynski@polsl.pl
* Correspondence: roman.korab@polsl.pl

Abstract: Photovoltaic (PV) systems are becoming increasingly popular, especially in residential buildings. However, the high penetration of prosumer PV micro-installations can have a negative impact on the operation of distribution networks due to the low self-consumption of the energy produced. One way to mitigate this problem is to use a residential energy storage system (RESS) and load shifting under a demand-side management (DSM) scheme. Energy management systems (EMSs) are used to control the operation of RESSs and to implement DSM. There are two main categories of EMSs: rule-based and optimization-based. Optimization-based EMSs provide better results than rule-based EMSs but can be computationally expensive. This article proposes an optimization-based EMS that is designed specifically for residential buildings. The proposed home energy management system (HEMS) uses a particle swarm optimization method to maximize the prosumer's financial neutrality, which is calculated based on dynamic energy prices. Simulation-based evaluation using the measurements taken in a building equipped with a PV source, RESS, and shiftable loads shows the improved performance of the proposed HEMS compared to rule-based RESS control. The results show that the designed HEMS increases self-consumption, thus reducing the impact of the prosumer's PV micro-installations on the distribution grid.

Keywords: photovoltaic micro-installation; residential building; prosumer; self-consumption; energy storage; load-shifting; home energy management system; dynamic energy prices; particle swarm optimization

check for updates

Citation: Korab, R.; Połomski, M.; Naczyński, T. Optimal Scheduling of Energy Storage and Shiftable Loads in Grid-Connected Residential Buildings with Photovoltaic Micro-Installations. *Energies* **2024**, *17*, 5264. https://doi.org/10.3390/en17215264

Academic Editor: Branislav Hredzak

Received: 27 September 2024
Revised: 17 October 2024
Accepted: 20 October 2024
Published: 23 October 2024

Copyright: © 2024 by the authors. Licensee MDPI, Basel, Switzerland. This article is an open access article distributed under the terms and conditions of the Creative Commons Attribution (CC BY) license (https://creativecommons.org/licenses/by/4.0/).

1. Introduction

Photovoltaic (PV) technology has evolved in recent decades into a major worldwide renewable generation technology [1]. By the end of 2022, the global cumulative installed capacity of PV systems reached 1177 GW and experienced 25% growth compared to 2021 [2]. Solar power contributes an increasing share of total electricity demand, accounting for 4.5% of global power production in 2022, up from 3.7% in the previous year. The reasons for this spectacular growth result from the unmatched versatility of PV technology, which can be applied in comparatively quickly deployed utility-scale projects at a competitive low cost and can generate energy for individual customers by means of rooftop micro-installations, increasing their self-sufficiency. Globally, the share of the rooftop segment has been growing continuously since 2018 and, in 2022, both marked segments were balanced, with 48% of new capacity on rooftops [3]. One of the markets with the fastest growing segment of rooftop PV installations is Poland, where the growth has been primarily driven by prosumer systems below 50 kW. In 2022, Poland's rooftop segment was responsible for 78% of the installed PV capacity. In the third quarter of 2023, there were more than

1,322,000 prosumer micro-installations in operation, with a total installed capacity of more than 10 GW [4].

The economy, combined with growing ecological awareness, is the most common factor in the decision to install a prosumer PV source [5]. On the other hand, the current regulatory framework favors self-consumption as the only economically viable model for rooftop PV installations [6]. Considering this, prosumers should select the rated power of their PV plants so that their annual generation is approximately equal to the annual electricity consumption of their households [7]. Since the capacity factor of the PV source is low (it ranges from 10% in Europe to 20% in Latin America [8], and in Poland, it is about 11% [9]), producing energy equal to the consumer's annual demand requires the installation of a PV source of sufficiently large power rating. With an average annual consumption in the EU household sector of 1671 kWh per capita [10], the power of a PV source should be equal to 1.9 kW per capita. The PV micro-installation capacity determined in this way is much larger than a typical household load [11]. In addition, load and generation profiles are usually divergent [12]. As a result, most of the energy produced is fed into the power system to be taken back from it later.

The high penetration of PV micro-installations can have a negative impact on the operation of distribution networks [13]. One way to eliminate it is to curtail the active power generation of PV sources when it becomes problematic. Smart inverters can first reduce the output power and may eventually shut down a micro-installation to mitigate adverse effects on the network [14]. However, this is an unfavorable remedy that limits the economic and environmental benefits of solar energy production. An alternative technique is to reduce the amount of energy injected by prosumers into the power system when the PV sources are operating by using a residential energy storage system (RESS) and load shifting under a demand-side management (DSM) scheme.

RESSs can decrease PV curtailment by storing excess generation and, therefore, can reduce the export of energy to the network [15]. Currently, battery-based energy storage systems are predominantly employed [16]. To maximize effectiveness, the battery should be charged during high PV production, when the risk of exceeding the normal operating conditions of the network is at its highest [17]. However, reducing PV curtailment is not the sole purpose of installing an RESS. An additional benefit of battery installation results from serving the household load with stored PV energy. Another option to decrease PV curtailment is DSM, which has the potential to be a practical solution in all energy demand sectors, including residential buildings [18]. In this case, DSM mostly refers to the active shifting of household loads to increase matching demand with the power production. To obtain the best results from the use of RESS and DSM, the prosumer should properly control the operation of the storage and flexible loads through an energy management system (EMS).

There are two main categories of EMSs [19]: rule-based EMSs and optimization-based EMSs. A rule-based EMS allocates the resources using predefined logical rules so that the energy produced can be adequately used or stored. An optimization-based EMS is more sophisticated and usually implements an optimization-based unit commitment (UC) model that considers several technical constraints while optimizing the objective function. The authors of article [19] compared these two approaches by controlling a microgrid testbed equipped with controllable load banks, a battery, a diesel genset, and wind energy as well as PV simulators and generators. Article [20], on the other hand, compared the employment of these methods to control the operation of a microgrid in an office building supplied by PV and wind sources, as well as by various storage units. In both cases, the optimization-based EMS minimized the operating costs of the microgrid. The optimization problem formulated in [19] has been decomposed into UC and optimal power flow (OPF) problems [21]. A mixed-integer linear programming (MILP) method was used to solve the UC problem, while the OPF problem was solved using an interior-point nonlinear programming method. The MILP method was also used in [20].

Articles [19,20] considered microgrids with relatively large source and load capacities. In turn, article [22] compared these methods to control the energy flexibility in a single residential building with PV. The flexible sources included were a heat pump with an auxiliary electric resistance heater and a water tank, a battery, and shiftable loads (SLs), such as washing machines. Under the rule-based control, the PV's self-consumption was maximized, and the building acted as a customer who actively tried to avoid supplying PV electricity to the grid and did so only when other options were unsuccessful. If there was surplus PV power available, the energy was self-consumed in the following priority: firstly, shiftable appliances were operated; secondly, the remaining surplus was stored in the battery; and lastly, the remaining surplus was converted to heat and stored. At times when the PV power did not cover all consumption, the battery was discharged, and only the deficit was drawn from the grid. The second control approach analyzed in [22] was the cost-optimal control, which minimizes the total electricity cost to the building. In this mode, the building takes the role of an active prosumer that both buys and sells electricity. The electricity cost is minimized over sequential 24 h horizons using a deterministic dynamic programming (DP) algorithm. A similar optimization algorithm was applied in the article [23], in which the battery's state of charge (SoC) was chosen as the decision variable to maximize the user's profit. The proposed optimization-based control method was compared with the rule-based method in simulations conducted for a residential building equipped with a PV source and storage unit. An analogous comparison was made in the paper [24], with the MILP method being used to optimally control the energy storage and heat pump. The objective was to minimize costs and peak power while considering the thermal comfort of the residents of the building.

In the articles discussed above, various objective functions and optimization algorithms were used to control EMSs. In each case, better results were obtained for optimization-based EMSs than for rule-based EMSs. However, when applying the optimization-based control, the computation time can be long [21] and is highly dependent on the flexible sources included [22] and the simulation time step assumed [23]. As a result, high-performance computing may be required. This may be a significant obstacle to implementing optimization-based control into EMSs in residential buildings. Therefore, it is necessary to search for optimization methods that provide adequate results without having such high computational requirements. This is the purpose of this article.

The remainder of this study is organized as follows. In Section 2, a method for the optimal control of RESSs and SLs that maximizes the prosumer's financial neutrality is proposed. Section 3 presents a test installation located in a residential building equipped with a rooftop PV source, an RESS, and controllable household appliances, where field measurements were taken to test and validate the proposed method. The simulation results are shown and discussed in Section 4. Section 5 describes the architecture and framework of the proposed optimization-based EMS. Finally, the main contributions of the presented work and the conclusion are given in Section 6.

2. Control Algorithm for Maximizing the Prosumer's Financial Neutrality

The above-mentioned challenges and current trends indicate the need to look for a simple, scalable system that can be widely applied in residential buildings in order to spread the concept of renewable energy based on PV technology. Of particular importance in this system is a method for adequately controlling the operation of RESSs and flexible loads, which consequently leads to the search for a suitable EMS system that, at its core, contains a dedicated algorithm whose task is to optimally control devices for a predetermined objective function. While rule-based management strategies continue to be developed and refined [25], management strategies using novel approaches based on various computational intelligence tools are gaining popularity and attention from researchers [26]. In particular, extensive applications of artificial intelligence techniques to hybrid microgrids based on renewable energy sources have been highlighted, addressing problems such as multi-criteria optimization, demand and supply forecasting, energy management [27], as

well as fault detection, classification, and security [28]. A variety of techniques have been applied in this regard, such as machine learning, genetic algorithms, neural networks, swarm intelligence methods, and others. Among these, the multi-agent metaheuristic algorithms, such as particle swarm optimization (PSO), are especially gaining in popularity.

PSO is a stochastic population-based meta-heuristic optimization method inspired by swarm intelligence, such as the social behavior of bird flocking. It mimics the cooperative behavior of birds in a flock, where individual birds work together to find food and protect themselves from predators. Its first application to optimization problems was proposed by Kennedy and Eberhart [29], and it has since been successfully applied in many fields [30].

In general, the optimization problem considered in this paper can be defined as:

$$\min_{\mathbf{x}} f(\mathbf{x}), \tag{1}$$

where $f : \mathbb{R}^N \to \mathbb{R}$ is the objective function, and vector $\mathbf{x} \in \mathbb{R}^N$ represents the problem's decision variables. The problem described by Equation (1) is treated as an unconstrained optimization problem. However, only solutions belonging to a subset of the search space are considered admissible. The feasible subset of the search space is defined as follows:

$$\mathbf{\Omega} = \left[x_1^l, x_1^u\right] \times \left[x_2^l, x_2^u\right] \times \cdots \times \left[x_N^l, x_N^u\right] \subset \mathbb{R}^N, \tag{2}$$

where x_j^l and x_j^u are, respectively, the lower and upper bounds of the search space along dimensions j, for $j = 1, 2, \ldots, N$, where N is the number of decision variables.

PSO employs a swarm of particles, each representing a potential solution to an optimization problem. In a swarm of size M, these potential solutions are denoted by the particles' current positions:

$$\mathbf{x}_i = [x_{i_1}, x_{i_2}, \ldots, x_{i_N}]^{\mathrm{T}}, \text{ for } i = 1, 2, \ldots, M, \tag{3}$$

where $\mathbf{x}_i$ is the position of the i-th particle. Each particle i, in addition to its position vector $\mathbf{x}_i$, also has a velocity vector $\mathbf{v}_i$, defined as:

$$\mathbf{v}_i = [v_{i_1}, v_{i_2}, \ldots, v_{i_N}]^{\mathrm{T}}, \text{ for } i = 1, 2, \ldots, M. \tag{4}$$

Additionally, the particles maintain the value of their most favorable personal position so far, represented by $\mathbf{p}_i$. The overall best position $\mathbf{g}$ found by any particle in the swarm, known as the swarm leader, is also tracked.

During the iterative optimization process, the best position of each particle $\mathbf{p}_i$ is maintained or updated. An update occurs when the particle's new position yields a smaller value of the objective function. For the i-th particle, the value of its personal best position $\mathbf{p}_i^k$ in the k-th iteration is updated according to the following rule:

$$\mathbf{p}_i^k = \begin{cases} \mathbf{x}_i^k & \text{if} \quad f(\mathbf{x}_i^k) < f(\mathbf{p}_i^{k-1}) \\ \mathbf{p}_i^{k-1} & \text{if} \quad f(\mathbf{x}_i^k) \geqslant f(\mathbf{p}_i^{k-1}) \end{cases}. \tag{5}$$

For iteration k, based on the personal best positions of all particles $\{\mathbf{p}_1^k, \mathbf{p}_2^k, \ldots, \mathbf{p}_M^k\}$, the swarm leader $\mathbf{g}$ is selected using the formula:

$$\mathbf{g}^k = \arg\min f\left(\{\mathbf{p}_i^k\}\right), \text{ for } i = 1, 2, \ldots, M, \tag{6}$$

where $\mathbf{g}^k$ represents the best position discovered by any of the particles at iteration k.

The algorithm proceeds iteratively and, during this process, particles traverse the search space, considering their individual optimal position as well as the collective best

position. The velocity and position of each particle are updated based on these factors. At iteration k, for each particle i, its velocity is updated first, using the following formula:

$$\mathbf{v}_i^{k+1} = \chi\left(\mathbf{v}_i^k + c_1\mathbf{r}_1^k\left(\mathbf{p}_i^k - \mathbf{x}_i^k\right) + c_2\mathbf{r}_2^k\left(\mathbf{g}^k - \mathbf{x}_i^k\right)\right). \tag{7}$$

The particle's velocity is then restricted to predetermined minimum and maximum values (v_{min} and v_{max}) [31], followed by updating its position:

$$\mathbf{x}_i^{k+1} = \mathbf{x}_i^k + \mathbf{v}_i^{k+1}, \quad i = 1, 2, \ldots, M, \tag{8}$$

where $\mathbf{r}_1$ and $\mathbf{r}_2$ are N-dimensional vectors of uniformly distributed random numbers within the range $[0, 1]$, c_1 and c_2 are acceleration coefficients, and χ is the so-called constriction factor [32]. Factors c_1 and c_2 determine the range of particle motion in an iteration. In most cases, they are identical.

In the optimization problem discussed in this article, each particle represents an RESS operating profile for an assumed 24 h time horizon. It also stores values representing the switching time of the SLs. This means that each particle has 25 elements (parameters), of which the first 24 elements represent the operating points of the RESS in the subsequent hours of the day, and the last element represents the time of switching on the SL (it was assumed that the SL can be switched on at any hour of the day, but its operation must be completed within the analyzed 24 h time horizon). During the optimization process, the PSO algorithm utilizes OpenDSS simulation software (version 9.6.1.1) [33], which uses a model of a building's power supply system implemented specifically for the purpose of the optimization procedure (the model is described in Section 3).

Figure 1 illustrates the sequence of steps of the PSO algorithm and how it interacts with the OpenDSS environment. During the algorithm initialization, an initial swarm (3) is generated. The values of swarm particles are randomly chosen from a set of permissible solutions. Furthermore, each particle is assigned a randomized initial velocity value (4). Then, during the initialization stage, the algorithm computes the objective function value for every particle, which also serves as its initial best value. Based on these, the swarm leader is determined (6). After the initialization step, the algorithm progresses to the iterative phase. In each iteration, after determining the velocity of the particles (7) and restricting them to their limiting values, new positions of the particles are calculated (8) while respecting their permissible values. Based on the new positions of the particles, the input OpenDSS model is modified. The primary algorithm initiates the simulation process, which is executed by the OpenDSS simulation engine. Based on the result of the simulations, an objective function value is calculated. Once the objective function values are determined, the best positions of each particle in the swarm are updated (5), and the leader of the swarm is selected (6). If the termination condition is not met, the algorithm will continue its operation in a loop, and the described process will be repeated.

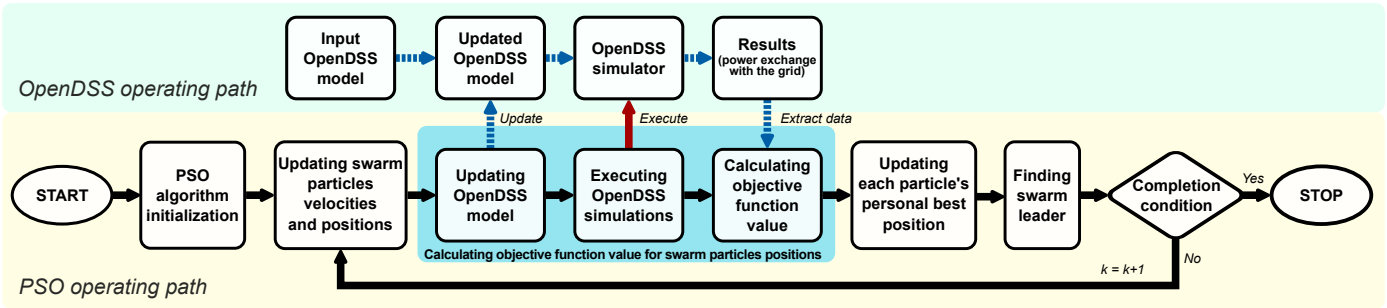

Figure 1. PSO-based optimization algorithm flowchart.

From the standpoint of the problem examined in this article, specifically the optimization of the operation of the RESS and SLs and the general optimization problem formulated

by Equation (1), it is crucial to properly define the objective function's form. According to the European Commission's regulation establishing a guideline on electricity balancing [34], the settlement processes should ensure the financial neutrality of all Transmission System Operators. An analogous principle was adopted in this article for the selection of the objective function for the problem of optimizing the operation of the RESS and SLs. It was assumed that the goal of the optimization was to maximize the daily financial neutrality of the prosumer. This could be achieved by minimizing the objective function f, defined by the formula:

$$f = \sqrt{\sum_{h=1}^{24} (c_h P_{\mathrm{EX},h})^2}, \tag{9}$$

where $P_{\mathrm{EX},h}$ is the power exchange with the grid in hour h, and c_h is the energy price in hour h. The value of the power exchange with the grid in hour h can be calculated using the following formula:

$$P_{\mathrm{EX},h} = P_{\mathrm{FIX},h} + P_{\mathrm{SHIFT},h} - P_{\mathrm{PV},h} - P_{\mathrm{RESS},h}, \tag{10}$$

where $P_{\mathrm{FIX},h}$ and $P_{\mathrm{SHIFT},h}$ are fixed and shiftable loads, respectively; $P_{\mathrm{PV},h}$ is the PV source generation; and $P_{\mathrm{RESS},h}$ is the energy storage operation point. The value of $P_{\mathrm{RESS},h}$ can be positive or negative (a positive sign indicates discharging, and a negative sign indicates charging the battery). Therefore, by controlling the operating point of RESS and the switching time of the SLs, it is possible to change the value of the power exchange with the grid in individual hours and, as a result, the value of the optimized objective function (9).

Dynamic energy prices, changing on an hourly basis, were assumed to be used in the calculations. This is the preferred method of settling transactions in the energy market in the European Union [35]. The 24 h horizon, on the other hand, is a realistic optimization horizon in terms of day-ahead electricity price and weather forecast availability. Dynamic energy prices can have a positive or negative value (negative energy prices indicate a general need to increase the flexibility of the power system; in the case of prosumers, this phenomenon should stimulate an increase in self-consumption, e.g., by storing energy or increasing load by switching on additional shiftable loads). Power exchange with the grid can also be positive (import from the grid) or negative (export to the grid). As a result, the products of price and power appearing in the formula (9) can also be positive or negative, representing cost or income (Table 1). By squaring these products, the prosumer's cost and income are both minimized. In this way, the prosumer's financial neutrality is maximized. The application of the square root ensures better convergence of the optimization algorithm.

Table 1. Combinations of energy price and power exchange with the grid resulting in a cost or income for the prosumer.

Quantity/Value		**Power Exchange with the Grid**	
		Positive	**Negative**
Energy price	Positive	Cost	Income
	Negative	Income	Cost

3. Overview of a Test Installation and Input Data

The simulations carried out to test the proposed optimization method were based on measurements taken in a real residential detached house located in southern Poland. The building was inhabited by four people, and the annual electricity consumption was approximately 5000 kWh. The house was equipped with a rooftop PV micro-installation with a rated power of 5.25 kW and a Li-ion battery RESS with a rated power of 5 kW and a capacity of 20.8 kWh. The battery minimum SoC was set to 10%, while the maximum SoC was 100%. There were typical electrical appliances in the household, among which, the washing machine, clothes dryer, and dishwasher could be used as SLs. Dedicated

energy meters were installed in the building's power supply system to monitor PV generation, storage operation, total load, and power exchange with the grid. The results of the measurements were recorded with a 1 min resolution.

Figures 2 and 3 show the operation of the building's power supply system for two consecutive weekdays in September 2023 (all figures in the article use Coordinated Universal Time or UTC; in the summer in Poland, local time is UTC +02.00). No central EMS was used when the measurements were taken, as the RESS was being controlled by its own rule-based algorithm that minimized the power exchange with the grid. In addition, no DSM was used during the measurements.

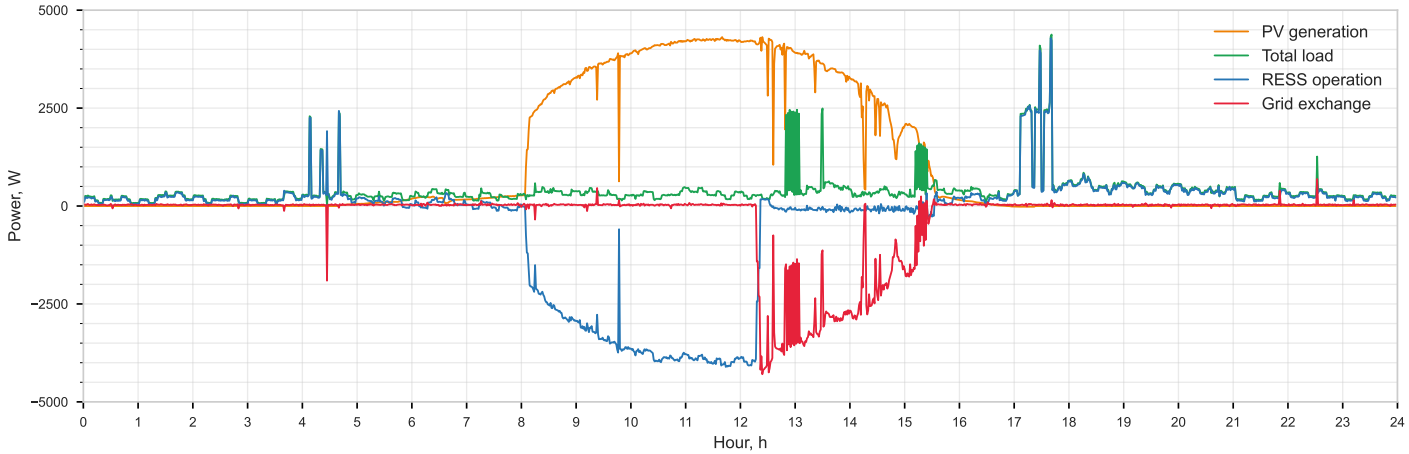

Figure 2. PV generation, total load, RESS operation, and power exchange with the grid on 20 September 2023, recorded at 1 min resolution in the analyzed residential building.

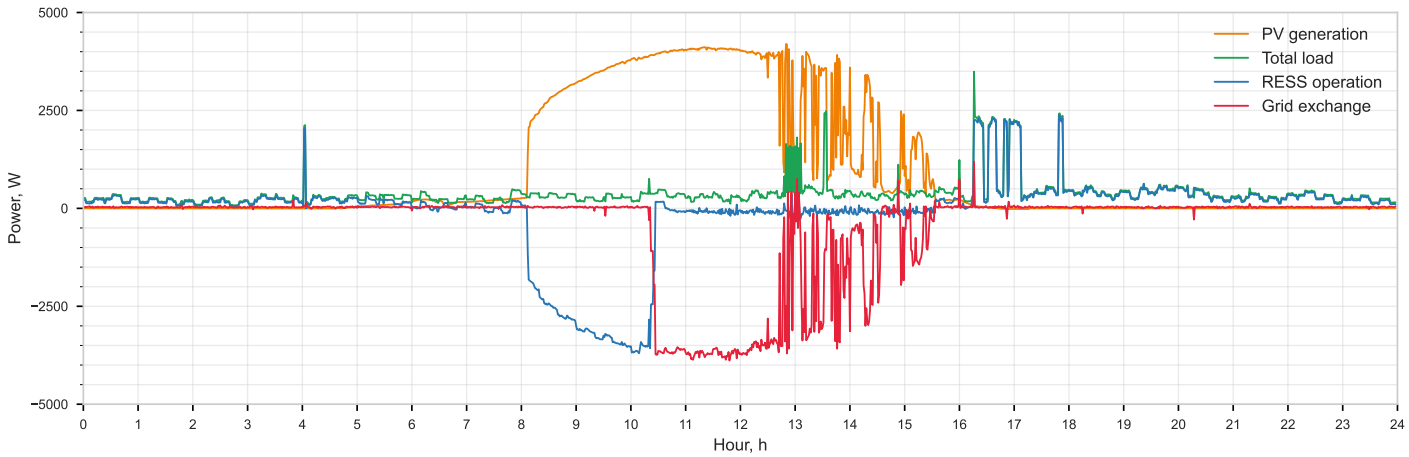

Figure 3. PV generation, total load, RESS operation, and power exchange with the grid on 21 September 2023, recorded at 1 min resolution in the analyzed residential building.

The days of 20 September (Wednesday) and 21 September (Thursday) were selected for evaluating the proposed optimization method due to their similar PV generation and load profiles. The operation of the RESS, which was fully charged around noon, was also similar. On both days, the operation of a potential SL could also be observed in the afternoon, after the PV source generation was completed. However, significant differences in the profiles of hourly electricity market prices were recorded on these days [36], as shown in Figure 4. The 21 September price profile had a typical shape, with stable prices during the day and higher prices in the evening peak. In contrast, the 20 September price profile showed a significant reduction in energy prices between 9 a.m. and 2 p.m., with negative prices between 10 a.m. and 1 p.m. This was the result of the high generation of renewable energy sources, particularly PV sources, during these hours [37]. The described common features

and differences for the chosen days allowed us to assess the impact of energy prices on the results of optimizing the operation of the RESS and SLs.

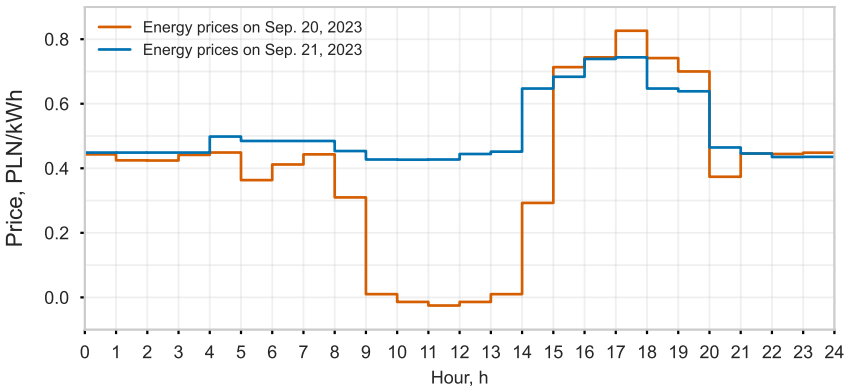

Figure 4. Hourly electricity market prices on 20 September and 21 September 2023 used in simulations (1 EUR is approximately 4.5 PLN).

Since electricity prices are quoted with an hourly resolution, all the simulations described in this article were carried out with an hourly resolution. The hourly energy balances also corresponded to the net-billing system, which was in use in Poland. Thus, the daily operating profiles of the building's power supply system recorded at 1 min resolution (Figures 2 and 3) had to be transformed to an hourly resolution. Hourly power values were determined in such a way that the hourly energy quantities for 1 min and hourly resolution were equal. Figures 5 and 6 show the recorded daily profiles transformed to hourly resolution. The power consumed by the electrical appliances (washing machine in Figure 5 and dishwasher in Figure 6), treated as SLs in the simulations, is marked with green bars.

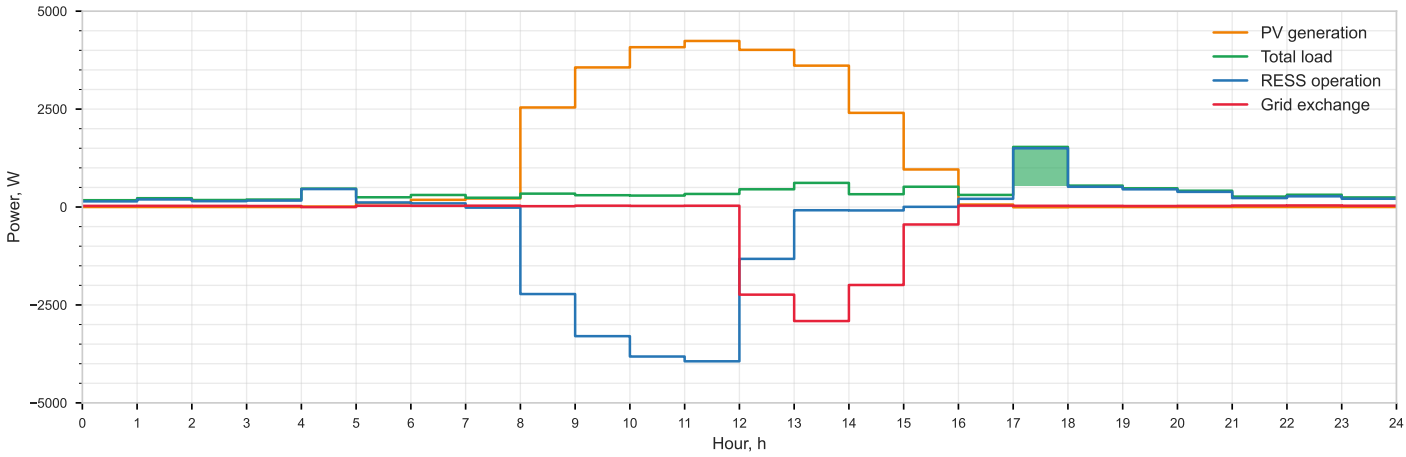

Figure 5. PV generation, total load, RESS operation, and power exchange with the grid on 20 September 2023, transformed to hourly resolution.

Simulations were carried out using a model of the building's power supply system implemented in OpenDSS software [33]. The model built in the OpenDSS environment considered the actual parameters of individual devices and their most important constraints, such as the SoC constraints for the RESS. An electrical topology in which the loads (shiftable and fixed), the RESS, and the PV source were connected to the single AC bus, which was directly connected to the low voltage (LV) grid, was employed (Figure 7). The measured operating profiles of the individual components of the building's power supply system were used to tune the model. During the simulations, the daily profiles of loads (fixed P_{FIX} and shiftable P_{SHIFT}), PV source generation (P_{PV}), energy storage operation

(P_{RESS}), and power exchange with the grid (P_{EX}) were recorded. The value of the objective function (9) was determined based on the recorded value of power exchanged with the grid (P_{EX}) and the hourly electricity prices shown in Figure 4. Simulations were carried out separately for the two days analyzed, each time starting from the battery SoC resulting from the measurements.

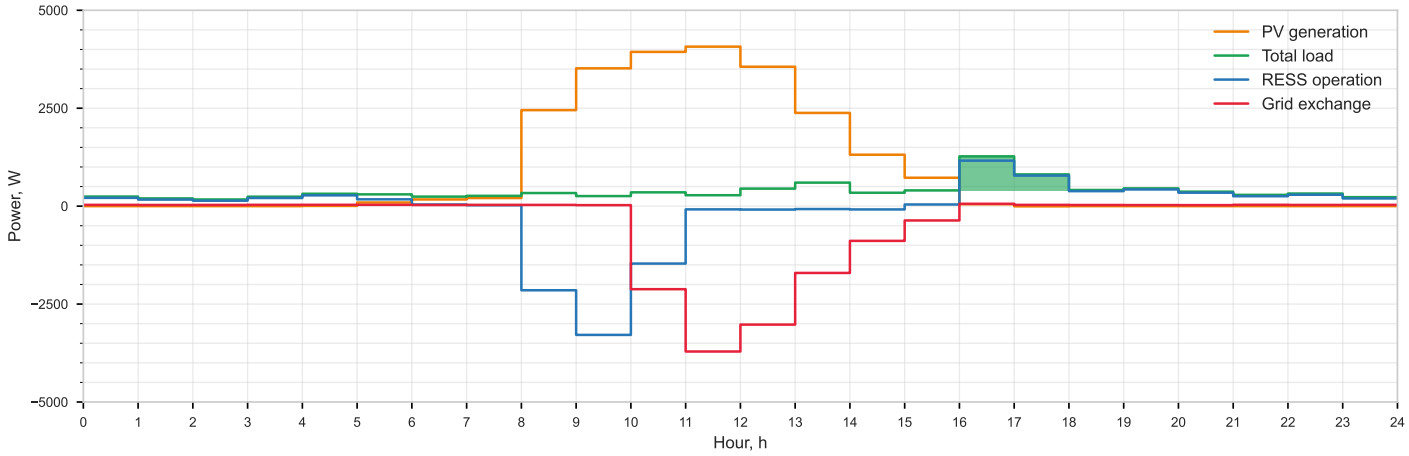

Figure 6. PV generation, total load, RESS operation, and power exchange with the grid on 21 September 2023, transformed to hourly resolution.

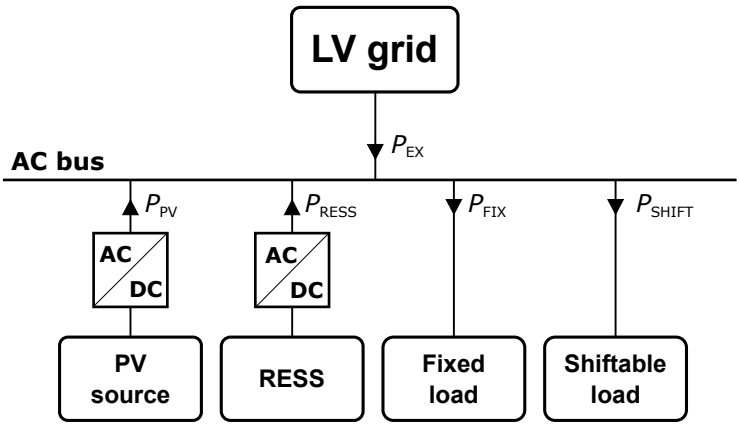

Figure 7. Building's power supply system model applied in simulations.

4. Simulation Results and Discussion

Two variants of the simulation were carried out to test the proposed optimization algorithm for each of the days analyzed. In the first variant, only the daily operation of the RESS was optimized, while in the second variant, both the operation of the RESS and the switching time of the SLs were optimized. Figure 8 shows the daily operating profiles of the RESS determined using the PSO algorithm, while Figure 9 shows the SoC of the storage. For comparison, the measured values of these quantities, resulting from the RESS control based on a factory-implemented rule-based algorithm, are also shown. Figure 10, on the other hand, shows the total load in the building, both measured and after optimizing the switching time of the SLs.

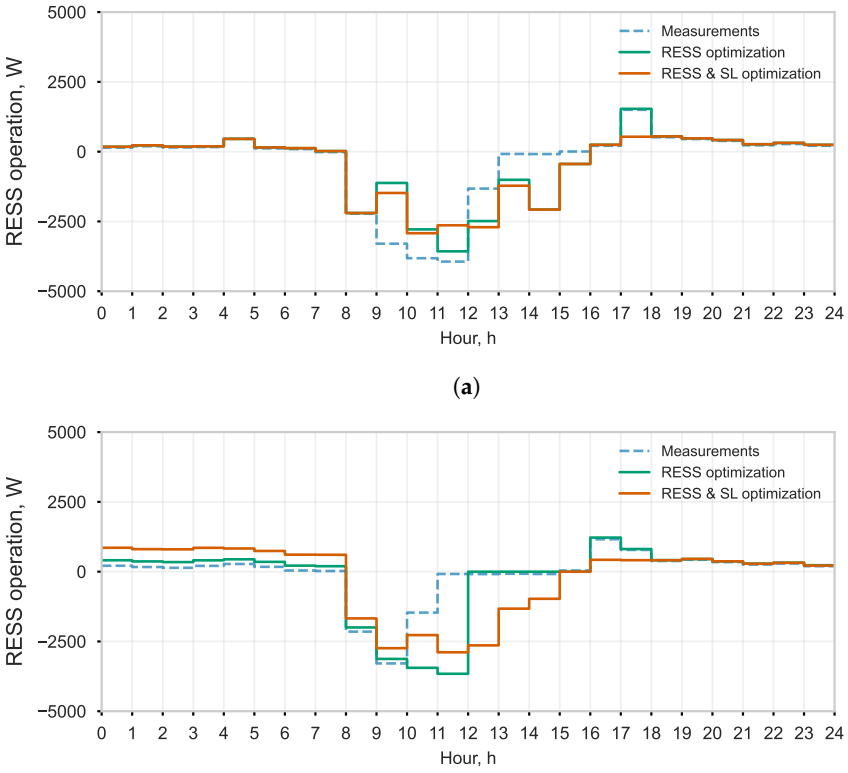

Figure 8. The measured and optimized daily operating profiles of the RESS (**a**) on 20 September 2023 and (**b**) on 21 September 2023.

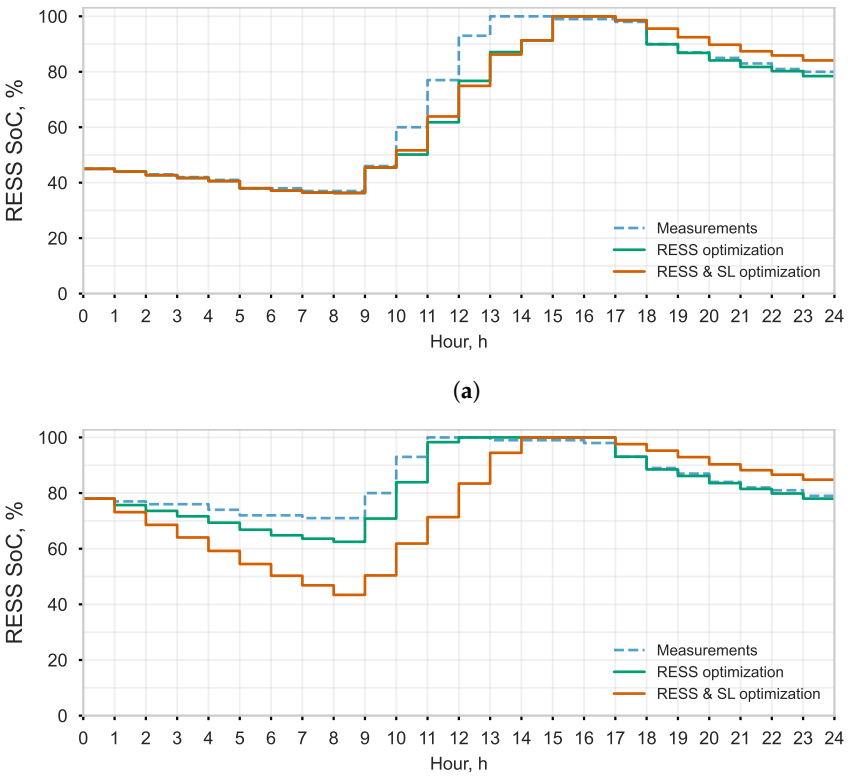

Figure 9. RESS SoC resulting from the measured and optimized operating profiles of the RESS (**a**) on 20 September 2023 and (**b**) on 21 September 2023.

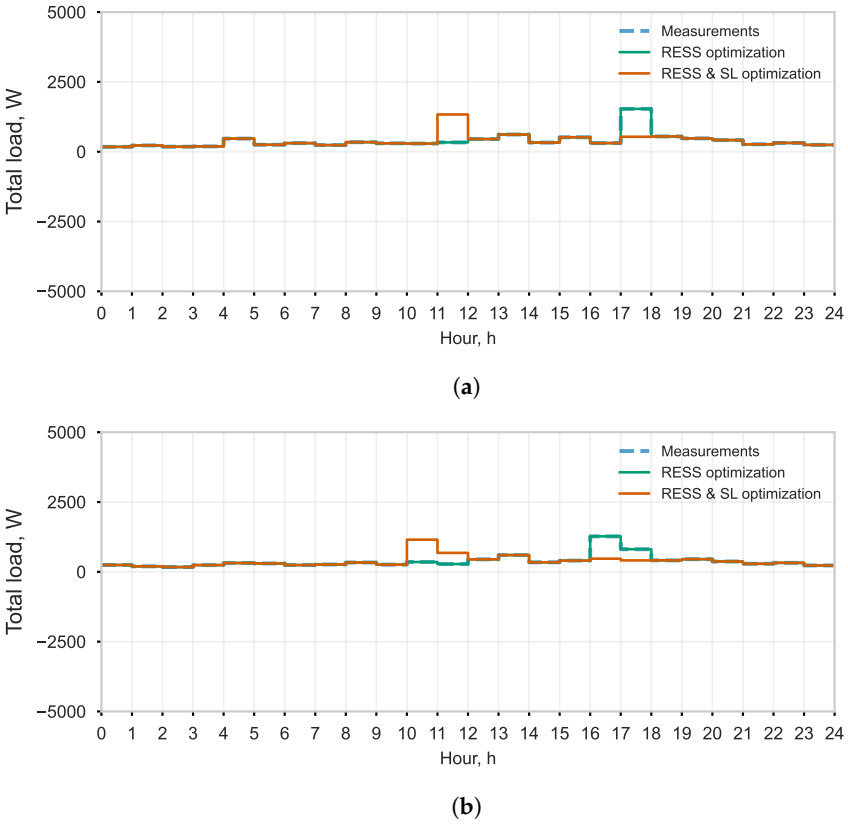

Figure 10. The measured and optimized total load of the residential building (**a**) on 20 September 2023 and (**b**) on 21 September 2023.

On 20 September (a day with negative energy prices), from midnight to 9 a.m., the RESS operation determined by the optimization algorithm (in both variants) was the same as the RESS operation recorded at that time (Figure 8a). Also, in the evening and the first part of the following night, the optimization results coincided with the measurements. The major differences in storage operation occurred between 9 a.m. and 3 p.m., i.e., during the period when energy prices were low. From 9 a.m. to 12 p.m., the RESS charging power calculated by the PSO algorithm was lower than the charging power resulting from the measurements. Controlling the storage in this way allowed it to operate in charging mode for a longer time compared to the situation when the storage was controlled by a rule-based algorithm (Figure 9a). As a result, the operation of the RESS was better adapted to the generation profile of the PV source.

On the second analyzed day, 21 September, differences in the RESS operating profile determined by the PSO algorithm and the measured profile were already noticeable at night (Figure 8b). During this period, the PSO algorithm controlled the RESS to operate in the discharge mode with a higher power than the power determined by the rule-based algorithm. Part of the discharged energy was used to cover the building's demand, while the remaining part was supplied to the grid. This was beneficial for both the power system and the prosumer. Discharging the RESS with a higher power at night reduces the power generated from non-renewable resources. At the same time, the RESS became better prepared to operate in charging mode during the day (Figure 9b), when energy was generated by the PV source, which was noticeable around noon. On both the days analyzed, the effect of shifting load from evening to late morning hours on the operation of the RESS was also evident. During the hours when the demand in the building had increased (Figure 10), the RESS was charged with lower power, and the capacity saved in this way was utilized at other times.

A measurable effect of optimizing the RESS and the SL was to increase the self-consumption of energy produced by the PV source compared to the situation when the

storage was controlled by a rule-based algorithm. This is shown in Figure 11. After the application of the PSO, on the first analyzed day (Figure 11a), the self-consumption admittedly decreased from 9 a.m. to 12 p.m., but it was higher in the remaining hours in relation to the measurements. As a result, the total daily self-consumption increased from 43.1% to 46.9% after optimizing the RESS operation (Table 2). On the other hand, after optimizing the RESS and SL, the daily self-consumption increased to 48.0%. An even greater increase in self-consumption was recorded on 21 September (Figure 11b). On that day, the daily self-consumption increased from 36.7% when controlling the RESS with a rule-based algorithm to 41.8% after applying PSO. There was a further increase to 48.5% after optimizing storage and shiftable load.

Table 2. The daily performance of the analyzed residential building's power supply system, both measured and resulting from the application of PSO.

Results Obtained with:	PV Generation	Load	RESS Operation		Grid Exchange		Self-Consumption	Objective Function
			Charge	Discharge	Import	Export		
	kWh	kWh	kWh	kWh	kWh	kWh	%	PLN
20 September 2023								
Measurements	26.0	9.3	14.8	5.1	0.6	7.6	43.1	−0.65
RESS optimization	26.0	9.3	15.7	5.6	0.0	6.6	46.9	0.00
RESS & SL optimization	26.0	9.3	15.7	4.6	0.0	5.6	48.0	0.00
21 September 2023								
Measurements	22.5	9.1	7.2	5.1	0.6	11.8	36.7	−5.12
RESS optimization	22.5	9.1	12.2	6.8	0.0	7.9	41.8	−3.84
RESS & SL optimization	22.5	9.1	14.5	9.0	0.0	7.8	48.5	−3.64

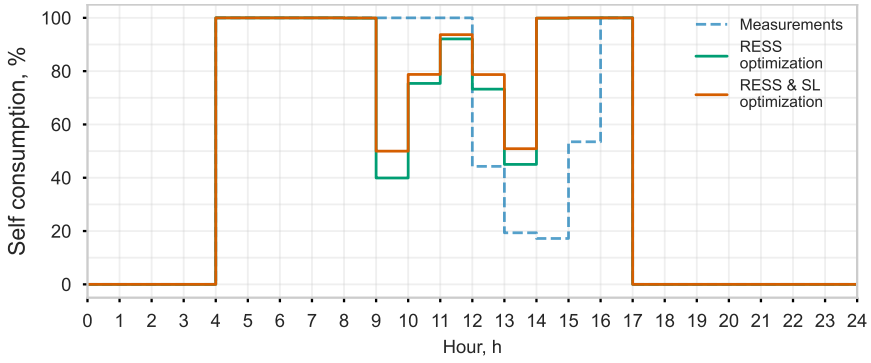

(**a**)

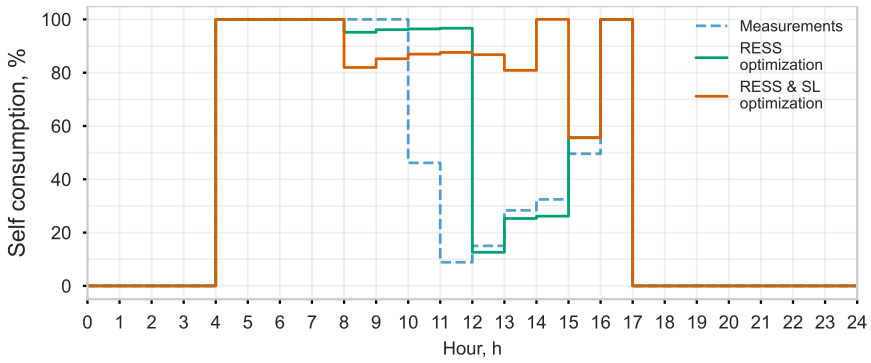

(**b**)

Figure 11. Self-consumption of PV energy resulting from the measured and optimized operating profiles of the RESS and SL (**a**) on 20 September 2023 and (**b**) on 21 September 2023.

A change in the level of self-consumption affects the exchange of energy with the LV distribution network. This is illustrated in Figure 12. After the application of PSO, only the export of energy to the grid occurred. On 20 September (Figure 12a), energy exports occurred for five hours, from 9 a.m. to 2 p.m., with a clear trend of reduction during hours when PV generation was higher. This phenomenon was closely related to the level of energy prices during these hours. From 9 a.m. to 10 a.m. and from 1 p.m. to 2 p.m., energy prices were at their highest and amounted to 0.01 PLN/kWh. From 10 a.m. to 11 a.m. and from 12 p.m. to 1 p.m., the prices dropped to −0.01 PLN/kWh, and from 11 a.m. to 12 p.m., the price was −0.02 PLN/kWh. Thus, to reduce the costs incurred by the prosumer as a result of the energy exports during hours when prices were negative, the PSO algorithm adequately reduced the exchange with the grid. This means that, when using an optimization-based EMS, energy prices can be an appropriate tool to influence the operating profiles of the RESS and the SL and, thus, the value of power exchanged with the grid. After optimizing the RESS operating profile, on 20 September, the daily energy export to the grid decreased from 7.6 kWh to 6.6 kWh (Table 2). The use of DSM further reduced it by 1 kWh. An even more pronounced reduction in the amount of energy exported to the grid as a result of PSO application was recorded on 21 September (Figure 12b). On that day, export to the grid decreased from 11.8 kWh to 7.9 kWh in the first optimization variant and to 7.8 kWh in the second variant.

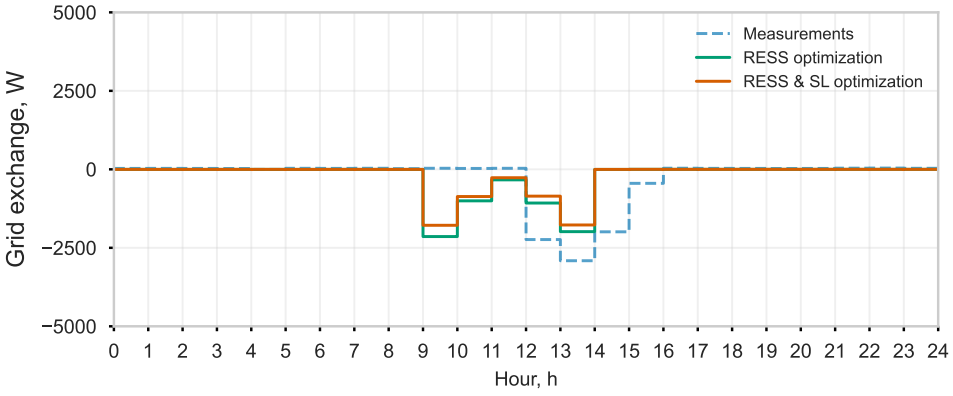

(**a**)

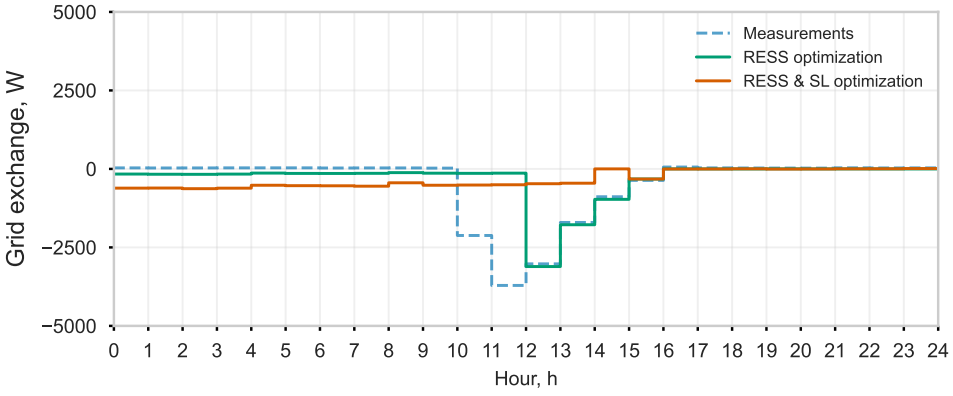

(**b**)

Figure 12. Power exchange with the grid resulting from the measured and optimized operating profiles of the RESS and SL (**a**) on 20 September 2023 and (**b**) on 21 September 2023.

In the method applied to optimize the operation of RESS and SL, it was assumed that the objective function was to maximize the daily financial neutrality of the prosumer. This required minimizing both cost and income. The results of the calculations are shown in Figure 13 (positive values represent the cost for the prosumer, and negative values

represent their income). On 20 September (Figure 13a), the prosumer earned income or incurred a cost only from 9 a.m. to 2 p.m., as there is no exchange of energy with the grid during the remaining hours. However, since energy prices were close to zero at this time, the income generated and the costs incurred were negligible and offset each other. As a result, complete financial neutrality of the prosumer was achieved on that day. The situation was slightly different on the next analyzed day. On 21 September (Figure 13b), after applying the PSO, the prosumer did not incur any costs, since the import of energy from the grid was zero and the energy prices on that day were exclusively positive. Instead, the prosumer received income for the energy sold. However, after optimization, the total daily income was approximately 25% lower than in the case when the RESS was controlled by a rule-based algorithm. Thus, the financial neutrality of the prosumer also increased on that day. A summary of the analysis results for both days is shown in Table 2. Detailed results are given in Appendix A (Tables A1–A6).

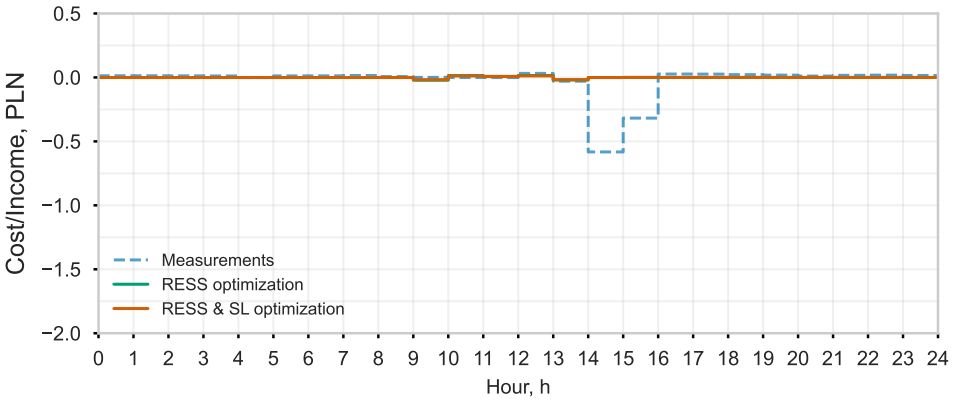

(**a**)

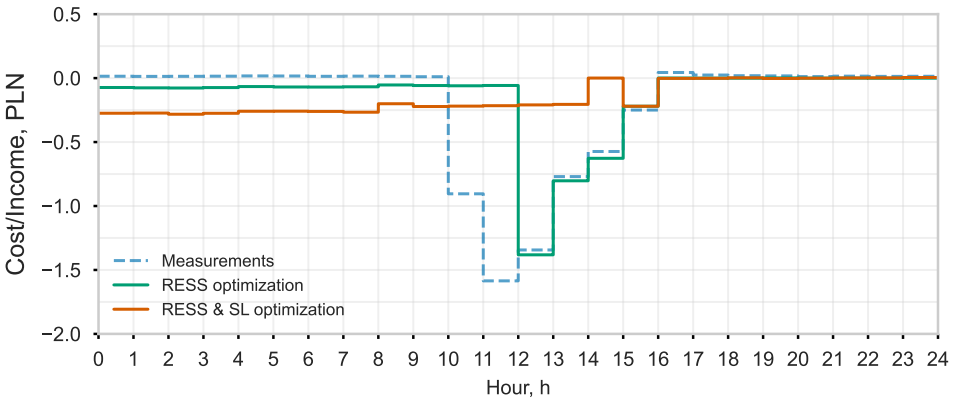

(**b**)

Figure 13. The prosumer's cost (positive values) and income (negative values) calculated based on measured and optimized power exchange with the grid (**a**) on 20 September 2023 and (**b**) on 21 September 2023.

When carrying out the simulations described above, a series of experiments were performed to observe the convergence process of the PSO algorithm. Figure 14 shows the results of the subsequent 10 daily PSO-optimized operating profiles of the RESS on 20 September 2023 (the daily operating profiles of the RESS shown in Figure 8 are the average of the 10 PSO optimizations). Additionally, the convergence curves of the PSO algorithm executions for the corresponding RESS optimization results displayed in Figure 14 are shown in Figure 15. The curves show decreasing values of the objective function for the swarm leader of each PSO run in successive iterations. A swarm of 40 particles was used for

these experiments. The PSO algorithm's parameter values χ and c_1, c_2 were experimentally selected and set to $\chi = 0.73$ and $c_1 = c_2 = 2.25$. The average duration of a single PSO optimization, obtained from 30 test runs, was approximately 22 s, with the maximum number of iterations set at 320. All simulations were carried out on a computer with an Intel Core i7-3770K CPU, 3.5 GHz with 16 GB of RAM, running on a 64-bit Windows 10 operating system.

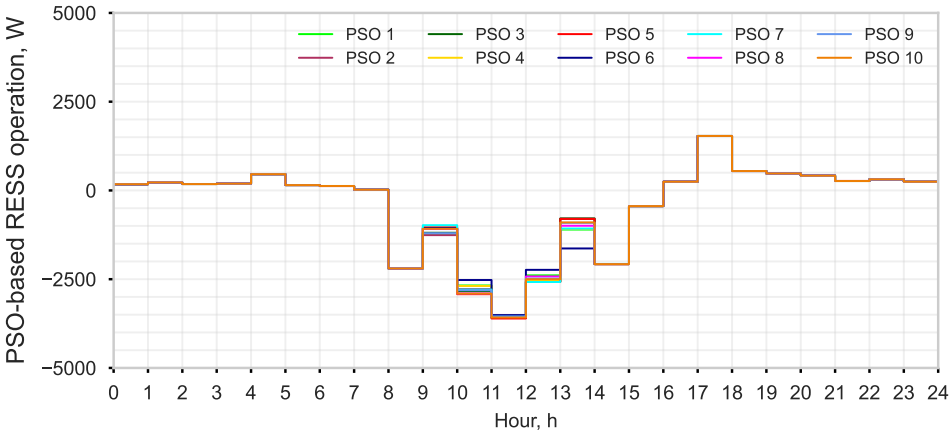

Figure 14. Results of the subsequent 10 PSO-based optimizations of the RESS operating profiles on 20 September 2023.

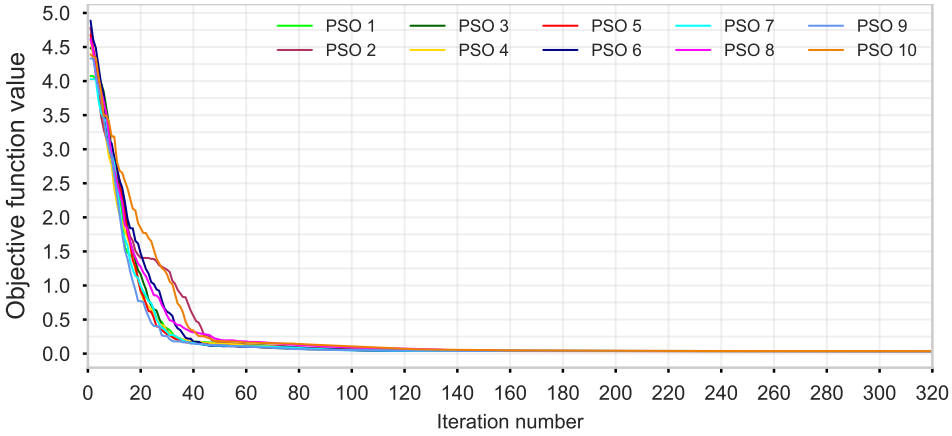

Figure 15. Convergence curves for 10 consecutive runs of the PSO algorithm obtained for the RESS optimization variant.

5. Home Energy Management System Architecture

An EMS designed to improve the energy management of residential buildings by controlling and scheduling the use of household equipment is called a home energy management system (HEMS) [38]. Figure 16 shows the HEMS architecture applying the proposed PSO-based method to optimize the operating profiles of the RESS and the SLs. This is a typical HEMS architecture [39], containing various household appliances, a PV source, an RESS, an electric vehicle, and a central controller. Household appliances are divided into conventional appliances, which require a smart plug, and smart appliances. The central controller is the core component of HEMS, and it optimizes and controls the energy usage in the household. Wired and wireless systems are used for communication between the corresponding devices. A human–machine interface (HMI) displays information from the controller, smart meters, sensors, smart plugs, and the smart appliances of the HEMS.

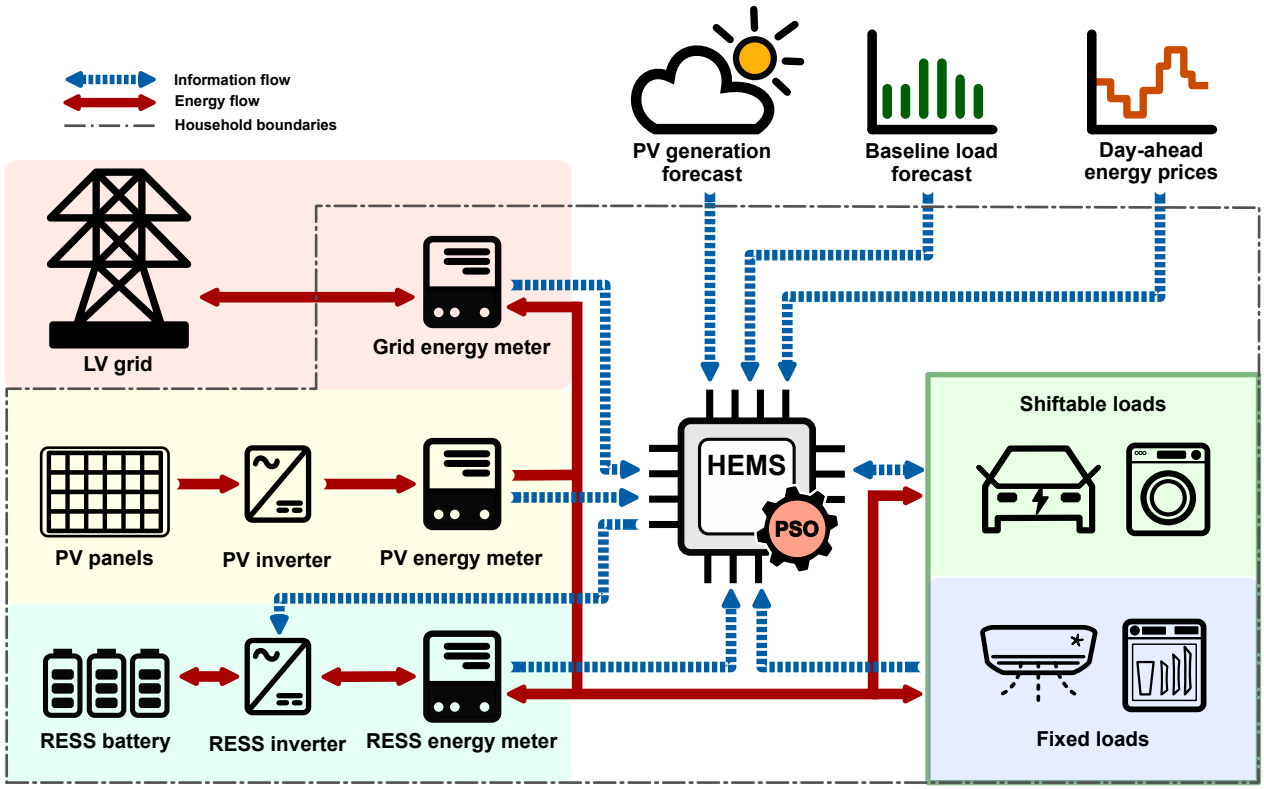

Figure 16. The HEMS architecture applying the proposed PSO-based method to optimize the operating profiles of the RESS and SLs.

The HEMS shown in Figure 16 is in the implementation stage in the residential building where the measurements used in this article were taken. A second analogous HEMS is being implemented in a similar building, also equipped with a PV source, RESS, and SLs. The designed HEMS will operate according to the following principles. At the planning stage, the central controller will collect information on the day-ahead energy prices, the PV source generation forecast, the building's baseline demand forecast, and the storage's SoC. The PV generation forecast will be based on numerical weather forecasts [40]. The building's baseline demand forecast will be determined using historical load profiles [41]. Using the HMI, the user will enter information into the system about the time intervals in which SLs can be switched on. The planned operating programs of these appliances will also be provided, and HEMS will download appropriate load profiles from the database containing data analogous to the load profiles described in [42]. Based on the described input data, the PSO algorithm implemented in the central controller will determine the RESS operating profile and the times of switching on the SLs. The proposed HEMS will use a moving horizon of 24 h. The operating schedule will be updated in accordance with the update time of numerical weather forecasts. During the implementation of the developed plan, data from energy meters will be recorded. In this way, the results of the applied forecasting and optimization methods will be verified and improved.

The practical implementation of HEMS in a real environment such as a residential building requires meeting several challenges, both technical and non-technical in nature. The first issue that determines the quality of the decisions developed by the HEMS is to ensure the highest possible accuracy of generation and load forecasts in the building. Other technical challenges include the need to equip many electrical devices with monitoring and control systems and to build a reliable communication system, which must also ensure a correspondingly high level of cybersecurity. An additional problem may be the need to integrate devices from different manufacturers, operating according to different communication standards or having no communication system at all, which directly affects the cost of system implementation. In turn, a non-technical challenge is the need to

raise awareness of people in the field of energy use and conservation so that residents of buildings equipped with HEMS will more willingly accept a situation in which some decisions are not made by them but by an automatic control system. It is obvious that the acceptance of such a situation will be easier for the residents when the decisions made by the HEMS system do not reduce their living comfort. This is another challenge that should be considered at the HEMS design and implementation stage.

6. Conclusions

The application of PV micro-installations to cover the electric energy needs of residential buildings is becoming increasingly popular worldwide. Unfortunately, the discrepancy between generation and load profiles results in low self-consumption, which means that a large part of the generated energy is transmitted to the LV grid, negatively affecting its operation. The remedy for this problem may be the use of RESSs and the implementation of DSM schemes, which involves switching on SLs at the appropriate time. However, such an extensive power supply system for a building requires a properly designed HEMS.

In this study, a PSO-based method was proposed to optimize the operation of an RESS and the switching time of SLs. The objective was to maximize the prosumer's financial neutrality, which was calculated based on dynamic energy prices. The proposed optimization method was validated using measurement results taken in a building equipped with an RESS controlled by a rule-based algorithm. Compared to the situation when the RESS was controlled by the rule-based algorithm, the simulation results demonstrated an increase in the self-consumption of produced energy. After the application of PSO, the total daily self-consumption increased from 43.1% to 46.9% on the first analyzed day and from 36.7% to 41.8% on the second day. An even greater increase was recorded after optimizing the RESS and SLs. In this case, the self-consumption increased to 48.0% on the first day and to 48.5% on the second day.

The increase in self-consumption affects the exchange of energy with the LV distribution grid. After optimizing the RESS operating profile, on the first analyzed day, the daily energy export to the grid decreased from 7.6 kWh to 6.6 kWh (13%), while on the second day it decreased from 11.8 kWh to 7.9 kWh (33%). The use of DSM further reduced the daily energy export to the grid. In addition, the proposed PSO-based algorithm also optimized the amount of energy exported to the grid at specific hours of the day, reducing exports at a time when PV generation was at its highest. This was particularly noticeable on the day with negative energy prices that occurred as a result of excess energy from renewable sources across the power system. This means that, using the proposed PSO-based HEMS, it is possible to use price signals from the wholesale energy market to control the operation of the individual RESS and the SLs in a way that improves the LV network operating conditions. Therefore, the proposed algorithm not only benefits the prosumer by maximizing self-consumption, but it also decreases the investment pressure on the distribution system operator by minimizing the negative grid impact of the prosumer's PV micro-installations. The proposed architecture of the HEMS is generic and practically applicable to any residential building, so it can be widely implemented in such locations.

Further research will include the integration of other renewable energy sources (e.g., wind microturbines) and electric appliances used to ensure thermal comfort in the building (heat pump, air conditioning, heat storage) into the HEMS system. The effects of controlling the prosumer power supply system according to other objective functions (e.g., cost minimization) will also be analyzed, and the impact of different control strategies on the operation of the low-voltage distribution network will be compared.

Author Contributions: Conceptualization, R.K.; methodology, R.K., M.P. and T.N.; validation, R.K., M.P. and T.N.; formal analysis, R.K., M.P. and T.N.; investigation, R.K., M.P. and T.N.; resources, R.K., M.P. and T.N.; data curation, R.K., M.P. and T.N.; writing—original draft preparation, R.K. and M.P.; writing—review and editing, R.K., M.P. and T.N.; visualization, M.P. and R.K.; PSO-based optimization algorithm design and implementation, M.P.; supervision, R.K. All authors have read and agreed to the published version of the manuscript.

Funding: This research received no external funding.

Data Availability Statement: The original contributions presented in the study are included in the article, further inquiries can be directed to the corresponding author.

Conflicts of Interest: The authors report no conflicts of interest.

Abbreviations

The following abbreviations are used in this manuscript:

DP	Dynamic Programming
DSM	Demand-Side Management
EMS	Energy Management System
HEMS	Home Energy Management System
MILP	Mixed-Integer Linear Programming
OPF	Optimal Power Flow
PSO	Particle Swarm Optimization
PV	Photovoltaic
RESS	Residential Energy Storage System
UC	Unit Commitment
SoC	State of Charge
LV	Low Voltage
SL	Shiftable Load
HMI	Human–Machine Interface

Appendix A

Here we present detailed results of the daily performance of the analyzed residential building's power supply system, both measured and resulting from the application of PSO. A positive value of grid exchange indicates import energy from the grid, while negative value indicates export energy to the grid. A positive value of RESS power indicates discharging, and a negative value indicates charging of the battery.

Table A1. The daily performance of the analyzed residential building's power supply system on 20 September 2023—measurements.

Hour	Price	PV Generation	Load	RESS Operation	SoC	Grid Exchange	Self-Consumption	Objective Function
	PLN/kWh	Wh	Wh	Wh	%	Wh	%	PLN/h
0	0.4431	0	174	144	45	30	0	0.0131
1	0.4246	0	225	194	44	31	0	0.0131
2	0.4241	0	179	149	43	29	0	0.0124
3	0.4415	0	190	164	42	26	0	0.0116
4	0.4489	12	469	459	41	−2	100	−0.0010
5	0.3633	100	249	116	38	33	100	0.0120
6	0.4118	184	308	93	38	30	100	0.0125
7	0.4431	219	237	−16	37	34	100	0.0151
8	0.3098	2541	342	−2222	37	22	100	0.0067
9	0.0100	3564	301	−3297	46	34	100	0.0003
10	−0.0141	4080	292	−3817	60	29	100	−0.0004
11	−0.0252	4239	334	−3939	77	33	100	−0.0008
12	−0.0141	4012	453	−1324	93	−2237	44	0.0316
13	0.0100	3609	616	−82	100	−2911	19	−0.0291
14	0.2927	2404	327	−87	100	−1990	17	−0.5825
15	0.7134	959	518	5	99	−446	53	−0.3180
16	0.7437	63	309	210	99	36	100	0.0266
17	0.8262	0	1534	1500	98	31	0	0.0258
18	0.7415	0	547	517	90	30	0	0.0219
19	0.7000	0	478	452	87	26	0	0.0182
20	0.3737	0	416	387	85	29	0	0.0108
21	0.4456	0	266	228	83	37	0	0.0167
22	0.4443	0	314	273	81	40	0	0.0179
23	0.4484	0	245	211	80	33	0	0.0150

Table A2. The daily performance of the analyzed residential building's power supply system on 20 September 2023—RESS optimization.

Hour	Price	PV Generation	Load	RESS Operation	SoC	Grid Exchange	Self-Consumption	Objective Function
	PLN/kWh	Wh	Wh	Wh	%	Wh	%	PLN/h
0	0.4431	0	174	175	45	−1	0	−0.0005
1	0.4246	0	225	227	44	−2	0	−0.0008
2	0.4241	0	179	181	43	−2	0	−0.0008
3	0.4415	0	190	192	42	−1	0	−0.0006
4	0.4489	12	469	459	41	−1	100	−0.0006
5	0.3633	100	249	151	38	−2	100	−0.0008
6	0.4118	184	308	125	37	−1	100	−0.0005
7	0.4431	218	237	20	36	−2	100	−0.0007
8	0.3098	2542	342	−2197	36	−3	100	−0.0008
9	0.0100	3564	301	−1121	45	−2141	40	−0.0214
10	−0.0141	4080	292	−2784	50	−1004	75	0.0141
11	−0.0252	4239	334	−3570	62	−335	92	0.0085
12	−0.0141	4013	453	−2486	77	−1073	73	0.0152
13	0.0100	3609	616	−1009	87	−1985	45	−0.0198
14	0.2927	2404	327	−2074	91	−3	100	−0.0009
15	0.7134	959	518	−441	100	0	100	0.0001
16	0.7437	63	309	246	100	0	100	0.0000
17	0.8262	0	1534	1534	99	0	0	0.0000
18	0.7415	0	547	547	90	0	0	−0.0001
19	0.7000	0	478	478	87	0	0	0.0000
20	0.3737	0	416	416	84	0	0	0.0000
21	0.4456	0	266	266	82	0	0	0.0001
22	0.4443	0	314	314	80	0	0	0.0000
23	0.4484	0	245	244	78	0	0	0.0001

Table A3. The daily performance of the analyzed residential building's power supply system on 20 September 2023—RESS & SL optimization.

Hour	Price	PV Generation	Base Load	Shifted Load	Total Load	RESS Operation	SoC	Grid Exchange	Self-Consumption	Objective Function
	PLN/kWh	Wh	Wh	Wh	Wh	Wh	%	Wh	%	PLN/h
0	0.4431	0	174	0	174	175	45	−1	0	−0.0006
1	0.4246	0	225	0	225	227	44	−2	0	−0.0008
2	0.4241	0	179	0	179	180	43	−1	0	−0.0006
3	0.4415	0	190	0	190	192	42	−1	0	−0.0006
4	0.4489	12	469	0	469	458	41	−1	100	−0.0005
5	0.3633	100	249	0	249	151	38	−2	100	−0.0006
6	0.4118	184	308	0	308	125	37	−1	100	−0.0006
7	0.4431	218	237	0	237	20	36	−1	100	−0.0004
8	0.3098	2542	342	0	342	−2198	36	−1	100	−0.0005
9	0.0100	3564	301	0	301	−1480	45	−1782	50	−0.0178
10	−0.0141	4080	292	0	292	−2922	52	−866	79	0.0122
11	−0.0252	4239	334	1000	1334	−2638	64	−267	94	0.0067
12	−0.0141	4013	453	0	453	−2706	75	−854	79	0.0121
13	0.0100	3609	616	0	616	−1221	86	−1772	51	−0.0177
14	0.2927	2404	327	0	327	−2075	91	−2	100	−0.0006
15	0.7134	959	518	0	518	−441	100	0	100	0.0001
16	0.7437	63	309	0	309	246	100	0	100	−0.0001
17	0.8262	0	534	0	534	534	99	0	0	0.0000
18	0.7415	0	547	0	547	546	96	0	0	0.0001
19	0.7000	0	478	0	478	478	92	0	0	−0.0001
20	0.3737	0	416	0	416	416	90	0	0	0.0001
21	0.4456	0	266	0	266	266	87	0	0	0.0000
22	0.4443	0	314	0	314	313	86	0	0	0.0000
23	0.4484	0	245	0	245	245	84	0	0	−0.0001

Table A4. The daily performance of the analyzed residential building's power supply system on 21 September 2023—measurements.

Hour	Price	PV Generation	Load	RESS Operation	SoC	Grid Exchange	Self-Consumption	Objective Function
	PLN/kWh	Wh	Wh	Wh	%	Wh	%	PLN/h
0	0.4487	0	244	212	78	33	0	0.0147
1	0.4487	0	197	167	77	30	0	0.0135
2	0.4487	0	170	139	76	31	0	0.0141
3	0.4487	0	241	208	76	34	0	0.0151
4	0.4983	6	316	275	74	34	100	0.0171
5	0.4846	93	301	174	72	34	100	0.0165
6	0.4846	171	243	42	72	29	100	0.0141
7	0.4846	207	263	24	71	32	100	0.0154
8	0.4535	2451	335	−2148	71	31	100	0.0142
9	0.4272	3518	257	−3287	80	25	100	0.0108
10	0.4267	3938	352	−1466	93	−2120	46	−0.9047
11	0.4272	4072	279	−83	100	−3711	9	−1.5854
12	0.4443	3559	447	−87	100	−3024	15	−1.3436
13	0.4516	2380	600	−74	99	−1705	28	−0.7701
14	0.6471	1313	342	−84	99	−887	32	−0.5738
15	0.6836	725	402	42	99	−365	50	−0.2498
16	0.7388	49	1271	1161	98	60	100	0.0440
17	0.7438	0	810	780	93	32	0	0.0241
18	0.6471	0	412	383	89	29	0	0.0188
19	0.6385	0	453	426	87	27	0	0.0173
20	0.4645	0	369	343	84	26	0	0.0119
21	0.4458	0	288	254	82	34	0	0.0153
22	0.4349	0	322	291	81	31	0	0.0135
23	0.4354	0	229	197	79	33	0	0.0143

Table A5. The daily performance of the analyzed residential building's power supply system on 21 September 2023—RESS optimization.

Hour	Price	PV Generation	Load	RESS Operation	SoC	Grid Exchange	Self-Consumption	Objective Function
	PLN/kWh	Wh	Wh	Wh	%	Wh	%	PLN/h
0	0.4487	0	245	408	78	−164	0	−0.0734
1	0.4487	0	198	367	76	−170	0	−0.0761
2	0.4487	0	170	343	74	−172	0	−0.0774
3	0.4487	0	241	406	72	−165	0	−0.0740
4	0.4983	6	316	443	69	−133	100	−0.0661
5	0.4846	93	301	351	67	−143	100	−0.0694
6	0.4846	171	243	216	65	−144	100	−0.0700
7	0.4846	207	263	196	64	−140	100	−0.0680
8	0.4535	2451	335	−1998	62	−118	95	−0.0536
9	0.4272	3518	257	−3125	71	−136	96	−0.0581
10	0.4267	3938	352	−3445	84	−141	96	−0.0601
11	0.4272	4071	279	−3658	98	−135	97	−0.0576
12	0.4443	3559	447	−2	100	−3110	13	−1.3817
13	0.4516	2380	600	−2	100	−1778	25	−0.8029
14	0.6471	1313	342	−2	100	−969	26	−0.6271
15	0.6836	725	402	−2	100	−322	56	−0.2201
16	0.7388	49	1271	1221	100	1	100	0.0006
17	0.7438	0	810	811	93	−1	0	−0.0004
18	0.6471	0	412	413	88	−1	0	−0.0006
19	0.6385	0	453	451	86	2	0	0.0013
20	0.4645	0	369	370	84	0	0	0.0000
21	0.4458	0	288	288	81	0	0	0.0000
22	0.4349	0	322	324	80	−2	0	−0.0007
23	0.4354	0	230	230	78	−1	0	−0.0004

Table A6. The daily performance of the analyzed residential building's power supply system on 21 September 2023—RESS & SL optimization.

Hour	Price	PV Generation	Base Load	Shifted Load	Total Load	RESS Operation	SoC	Grid Exchange	Self-Consumption	Objective Function
	PLN/kWh	Wh	Wh	Wh	Wh	Wh	%	Wh	%	PLN/h
0	0.4487	0	244	0	244	857	78	−612	0	−0.2746
1	0.4487	0	197	0	197	806	73	−609	0	−0.2732
2	0.4487	0	170	0	170	800	69	−630	0	−0.2825
3	0.4487	0	241	0	241	854	64	−613	0	−0.2751
4	0.4983	6	316	0	316	831	59	−520	100	−0.2592
5	0.4846	93	301	0	301	742	54	−534	100	−0.2586
6	0.4846	171	243	0	243	609	50	−538	100	−0.2605
7	0.4846	207	263	0	263	606	47	−550	100	−0.2666
8	0.4535	2451	335	0	335	−1674	43	−442	82	−0.2004
9	0.4272	3518	257	0	257	−2741	50	−520	85	−0.2222
10	0.4267	3938	352	800	1152	−2272	62	−513	87	−0.2190
11	0.4272	4071	279	400	679	−2888	71	−505	88	−0.2157
12	0.4443	3559	447	0	447	−2640	83	−471	87	−0.2095
13	0.4516	2380	600	0	600	−1325	94	−455	81	−0.2054
14	0.6471	1313	342	0	342	−971	100	1	100	0.0005
15	0.6836	725	402	0	402	−2	100	−322	56	−0.2200
16	0.7388	49	471	0	471	425	100	−3	100	−0.0023
17	0.7438	0	410	0	410	412	98	−2	0	−0.0015
18	0.6471	0	412	0	412	409	95	3	0	0.0022
19	0.6385	0	453	0	453	458	93	−4	0	−0.0026
20	0.4645	0	369	0	369	371	90	−1	0	−0.0007
21	0.4458	0	288	0	288	285	88	3	0	0.0014
22	0.4349	0	322	0	322	317	87	5	0	0.0020
23	0.4354	0	229	0	229	218	85	11	0	0.0048

References

1. International Energy Agency. Renewable Energy Market Update. Outlook for 2023 and 2024. Available online: https://iea.blob.core.windows.net/assets/63c14514-6833-4cd8-ac53-f9918c2e4cd9/RenewableEnergyMarketUpdate_June2023.pdf (accessed on 11 September 2024).
2. Solar Power Europe. Global Market Outlook for Solar Power 2023–2027. Available online: https://www.solarpowereurope.org/insights/outlooks/eu-market-outlook-for-solar-power-2023-2027/detail (accessed on 11 September 2024).
3. International Energy Agency. Snapshot of Global PV Markets 2023. Available online: https://iea-pvps.org/wp-content/uploads/2023/04/IEA_PVPS_Snapshot_2023.pdf (accessed on 3 September 2024).
4. Polish Power Transmission and Distribution Association. Micro-Installations in Poland as of 30 September 2023. Available online: http://ptpiree.pl/energetyka-w-polsce/energetyka-w-liczbach/mikroinstalacje-w-polsce (accessed on 7 September 2024).
5. Żuk, P.; Żuk, P. Prosumers in Action: The Analysis of Social Determinants of Photovoltaic Development and Prosumer Strategies in Poland. *Int. J. Energy Econ. Policy* **2022**, *12*, 294–306. [CrossRef]
6. European Environment Agency. Energy Prosumers in Europe—Citizen Participation in the Energy Transition. Technical Report No 1/2022, EEA. 2022. Available online: https://www.eea.europa.eu/publications/the-role-of-prosumers-of (accessed on 6 September 2024).
7. Kurz, D.; Nowak, A. Analysis of the Impact of the Level of Self-Consumption of Electricity from a Prosumer Photovoltaic Installation on Its Profitability Under Different Energy Billing Scenarios in Poland. *Energies* **2023**, *16*, 946. [CrossRef]
8. Bolson, N.; Prieto, P.; Patzek, T. Capacity Factors for Electrical Power Generation from Renewable and Nonrenewable Sources. *Proc. Natl. Acad. Sci. USA* **2022**, *119*, e2205429119. [CrossRef] [PubMed]
9. Olczak, P. Comparison of Modeled and Measured Photovoltaic Microinstallation Energy Productivity. *Renew. Energy Focus* **2022**, *43*, 246–254. [CrossRef]
10. Eurostat. Electricity and Heat Statistics. Consumption of Electricity per Capita in the Households Sector. Available online: https://ec.europa.eu/eurostat/statistics-explained/index.php?title=Electricity_and_heat_statistics (accessed on 11 September 2024).
11. Azarova, V.; Cohen, J.J.; Kollmann, A.; Reichl, J. Reducing Household Electricity Consumption during Evening Peak Demand Times: Evidence from a Field Experiment. *Energy Policy* **2020**, *144*, 111657. [CrossRef]
12. Hummel, S.; Betzold, C.; Dentel, A. Impact of the Weather Forecast Quality on a MPC-driven Heat Pump Heating System. In Proceedings of the CLIMA 2022 Conference, Rotterdam, The Netherlands, 22–25 May 2022. [CrossRef]
13. Uzum, B.; Onen, A.; Hasanien, H.M.; Muyeen, S.M. Rooftop Solar PV Penetration Impacts on Distribution Network and Further Growth Factors—A Comprehensive Review. *Electronics* **2021**, *10*, 55. [CrossRef]

14. Sharma, V.; Haque, M.H.; Aziz, S.M.; Kauschke, T. Smart Inverter and Battery Storage Controls to Reduce Financial Loss Due to Overvoltage-Induced PV Curtailment in Distribution Feeders. *Sustain. Energy Grids Netw.* **2023**, *34*, 101030. [CrossRef]
15. Sharma, V.; Haque, M.H.; Aziz, S.M.; Kauschke, T. Reduction of PV Curtailment through Optimally Sized Residential Battery Storage. In Proceedings of the 2020 IEEE International Conference on Power Electronics, Drives and Energy Systems (PEDES), Jaipur, India, Jaipur, India, 16–19 December 2020; pp. 1–6. [CrossRef]
16. Kandari, R.; Neeraj, N.; Micallef, A. Review on Recent Strategies for Integrating Energy Storage Systems in Microgrids. *Energies* **2023**, *16*, 317. [CrossRef]
17. Korab, R.; Połomski, M.; Smołka, M. Evaluating the Risk of Exceeding the Normal Operating Conditions of a Low-Voltage Distribution Network Due to Photovoltaic Generation. *Energies* **2022**, *15*, 1969. [CrossRef]
18. Bakare, M.S.; Abdulkarim, A.; Zeeshan, M.; Shuaibu, A.N. A Comprehensive Overview on Demand Side Energy Management towards Smart Grids: Challenges, Solutions, and Future Direction. *Energy Inform.* **2023**, *6*, 4. [CrossRef]
19. Restrepo, M.; Cañizares, C.A.; Simpson-Porco, J.W.; Su, P.; Taruc, J. Optimization- and Rule-based Energy Management Systems at the Canadian Renewable Energy Laboratory Microgrid Facility. *Appl. Energy* **2021**, *290*, 116760. [CrossRef]
20. Kanwar, A.; Rodríguez, D.I.H.; von Appen, J.; Braun, M. A Comparative Study of Optimization- and Rule-Based Control for Microgrid Operation. In Proceedings of the Power and Energy Student Summit (PESS) 2015, Dortmund, Germany, 13–14 January 2015. [CrossRef]
21. Olivares, D.E.; Cañizares, C.A.; Kazerani, M. A Centralized Energy Management System for Isolated Microgrids. *IEEE Trans. Smart Grid* **2014**, *5*, 1864–1875. [CrossRef]
22. Salpakari, J.; Lund, P. Optimal and Rule-Based Control Strategies for Energy Flexibility in Buildings with PV. *Appl. Energy* **2016**, *161*, 425–436. [CrossRef]
23. Varzaneh, S.G.; Raziabadi, A.; Hosseinzadeh, M.; Sanjari, M.J. Optimal Energy Management for PV-integrated Residential Systems Including Energy Storage System. *IET Renew. Power Gener.* **2021**, *15*, 17–29. [CrossRef]
24. Gelleschus, R.; Böttiger, M.; Bocklisch, T. Optimization-Based Control Concept with Feed-in and Demand Peak Shaving for a PV Battery Heat Pump Heat Storage System. *Energies* **2019**, *12*, 2098. [CrossRef]
25. Ali, A.O.; Hamed, A.M.; Abdelsalam, M.M.; Sabry, M.N.; Elmarghany, M.R. Energy Management of Photovoltaic-Battery System Connected with the Grid. *J. Energy Storage* **2022**, *55*, 105865. [CrossRef]
26. Mahmood, D.; Latif, S.; Anwar, A.; Hussain, S.J.; Jhanjhi, N.Z.; Sama, N.U.; Humayun, M. Utilization of ICT and AI Techniques in Harnessing Residential Energy Consumption for an Energy-Aware Smart City: A Review. *Int. J. Adv. Appl. Sci.* **2021**, *8*, 50–66. [CrossRef]
27. Rojek, I.; Mikołajewski, D.; Mroziński, A.; Macko, M. Machine Learning- and Artificial Intelligence-Derived Prediction for Home Smart Energy Systems with PV Installation and Battery Energy Storage. *Energies* **2023**, *16*, 6613. [CrossRef]
28. Zulu, M.L.T.; Carpanen, R.P.; Tiako, R. A Comprehensive Review: Study of Artificial Intelligence Optimization Technique Applications in a Hybrid Microgrid at Times of Fault Outbreaks. *Energies* **2023**, *16*, 1786. [CrossRef]
29. Kennedy, J.; Eberhart, R. Particle Swarm Optimization. In Proceedings of the ICNN'95—International Conference on Neural Networks, Perth, WA, Australia, 27 November–1 December 1995; Volume 4, pp. 1942–1948. [CrossRef]
30. Gad, A.G. Particle Swarm Optimization Algorithm and Its Applications: A Systematic Review. *Arch. Comput. Methods Eng.* **2022**, *29*, 2531–2561. [CrossRef]
31. Kennedy, J.; Eberhart, R.C.; Shi, Y. *Swarm Intelligence*; Morgan Kaufmann Publishers Inc.: San Francisco, CA, USA, 2001; pp. 328–331.
32. Clerc, M.; Kennedy, J. The Particle Swarm—Explosion, Stability, and Convergence in a Multidimensional Complex Space. *IEEE Trans. Evol. Comput.* **2002**, *6*, 58–73. [CrossRef]
33. Electric Power Research Institute. OpenDSS—Electric Power Distribution System Simulator. Available online: https://www.epri.com/pages/sa/opendss (accessed on 20 September 2024).
34. Official Journal of the European Union. Commission Regulation (EU) 2017/2195 of 23 November 2017 Establishing a Guideline on Electricity Balancing. Available online: https://eur-lex.europa.eu/legal-content/EN/TXT/PDF/?uri=CELEX:32017R2195&from=LV (accessed on 11 September 2024).
35. Nouicer, A.; Kehoe, A.M.; Nysten, J.; Fouquet, D.; Hancher, L.; Meeus, L. The EU Clean Energy Package (Ed. 2020). 2020. Available online: https://fsr.eui.eu/publications/?handle=1814/68899 (accessed on 11 September 2024).
36. PSE S.A. Balancing Market Operation—Settlement Prices. Available online: https://www.pse.pl/web/pse-eng/data/balancing-market-operation/settlement-prices (accessed on 11 September 2024).
37. Maciejowska, K. Assessing the Impact of Renewable Energy Sources on the Electricity Price Level and Variability—A Quantile Regression Approach. *Energy Econ.* **2020**, *85*, 104532. [CrossRef]
38. Zafar, U.; Bayhan, S.; Sanfilippo, A. Home Energy Management System Concepts, Configurations, and Technologies for the Smart Grid. *IEEE Access* **2020**, *8*, 119271–119286. [CrossRef]
39. Han, B.; Zahraoui, Y.; Mubin, M.; Mekhilef, S.; Seyedmahmoudian, M.; Stojcevski, A. Home Energy Management Systems: A Review of the Concept, Architecture, and Scheduling Strategies. *IEEE Access* **2023**, *11*, 19999–20025. [CrossRef]
40. Korab, R.; Kandzia, T.; Naczyński, T. Short-Term Forecasting of Photovoltaic Power Generation. *Prz. Elektrotechniczny* **2023**, *97*, 31–37. [CrossRef]

41. Kychkin, A.V.; Chasparis, G.C. Feature and Model Selection for Day-Ahead Electricity-Load Forecasting in Residential Buildings. *Energy Build.* **2021**, *249*, 111200. [CrossRef]
42. Papadopoulos, T.; Barzegkar-Ntovom, G.; Kryonidis, G.; Doukas, D.; Marinopoulos, A.; Covrig, C.-F.; Kontis, E. High Resolution Profiles of Residential Appliances. IEEE Dataport. 18 February 2020. Available online: https://ieee-dataport.org/open-access/high-resolution-profiles-residential-appliances (accessed on 11 September 2024). [CrossRef]

Disclaimer/Publisher's Note: The statements, opinions and data contained in all publications are solely those of the individual author(s) and contributor(s) and not of MDPI and/or the editor(s). MDPI and/or the editor(s) disclaim responsibility for any injury to people or property resulting from any ideas, methods, instructions or products referred to in the content.